Synthesis and Characterisation of ν_3-Octahedral $[Ni_{36}Pd_8(CO)_{48}]^{6-}$ and $[Ni_{35}Pt_9(CO)_{48}]^{6-}$ Clusters Displaying Unexpected Surface Segregation of Pt Atoms and Molecular and/or Crystal Substitutional Ni/Pd and Ni/Pt Disorder

Cristina Femoni,[a] Maria Carmela Iapalucci,[a] Giuliano Longoni,*[a] Per H. Svensson,[a, b] Piero Zanello,[c] and Fabrizia Fabrizi de Biani[c]

Abstract: The synthesis and structure, as well as the chemical and electrochemical characterisation of two new ν_3-octahedral bimetallic clusters with the general $[Ni_{44-x}M_x(CO)_{48}]^{6-}$ (M = Pd, $x = 8$; M = Pt, $x = 9$) formula is reported. The $[Ni_{35}Pt_9(CO)_{48}]^{6-}$ cluster was obtained in reasonable yields (56% based on Pt) by reaction of $[Ni_6(CO)_{12}]^{2-}$ with 1.1 equivalents of Pt^{II} complexes, in ethyl acetate or THF as the solvent. The $[Ni_{36}Pd_8(CO)_{48}]^{6-}$ cluster was obtained from the related reaction with Pd^{II} salts in THF, and was isolated only in low yields (5–10% based on Pd), mainly because of insufficient differential solubility of its salts. The unit cell of the $[NBu_4]_6[Ni_{35}Pt_9(CO)_{48}]$ salt contains a substitutionally Ni–Pt disordered $[Ni_{24}(Ni_{14-x}Pt_x)Pt_6(CO)_{48}]^{6-}$ ($x = 3$) hexaanion. A combination of crystal and molecular disorder is necessary to explain the disordering observed for the Ni/Pt sites. The unit cell of the corresponding $[Ni_{36}Pd_8(CO)_{48}]^{6-}$ salt contains two independent $[Ni_{30}(Ni_{8-x}Pd_x)Pd_6(CO)_{48}]^{6-}$ ($x = 2$) hexaanions. The two display similar substitutional Ni–Pd disorder, which probably arises only from crystal disorder. The structure of $[Ni_{36}Pd_8(CO)_{48}]^{6-}$ establishes the first similarity between the chemistry of Ni-Pd and Ni-Pt carbonyl clusters. A comparison of the chemical and electrochemical properties of $[Ni_{35}Pt_9(CO)_{48}]^{6-}$ with those of the related $[Ni_{38}Pt_6(CO)_{48}]^{6-}$ cluster shows that surface colouring of the latter with Pt atoms decreases redox as well as protonation propensity of the cluster. In contrast, substitution of all internal Pt and two surface Ni with Pd atoms preserves the protonation behaviour and is only detrimental with respect to its redox aptitude. A qualitative rationalisation of the different surface-site selectivity of Pt and Pd, based on distinctive interplays of M–M and M–CO bond energies, is suggested.

Keywords: carbonyl ligands · cluster compounds · crystal disorder · electrochemistry · structure elucidation

Introduction

Most reported high-nuclearity Ni–Pd, Ni–Pt, and Pd–Pt carbonyl clusters exhibit a clear-cut site and composition preference of the Pd and Pt atoms that is illustrated by the stoichiometric and ordered structure of $[Ni_{13}Pd_{13}(CO)_{34}]^{4-}$,[1] $[Ni_{16}Pd_{16}(CO)_{40}]^{4-}$,[2] $[Ni_{26}Pd_{20}(CO)_{54}]^{6-}$,[2] $[Ni_{36}Pt_4(CO)_{45}]^{6-}$,[3,4] $[HNi_{38}Pt_6(CO)_{48}]^{5-}$,[5,6] $[Ni_{24}Pt_{14}(CO)_{44}]^{4-}$,[7] $[Ni_9Pd_{33}(CO)_{41}(PPh_3)_6]^{4-}$,[8] $[Ni_4Pd_{16}(CO)_{22}(PPh_3)_4]^{2-}$[9] and $[H_{12}Pd_{28}Pt_{13}(CO)_{27}(PMe_3)(PPh_3)_{12}]$.[10] In general, the structures of the above species show that interactions among similar atoms are maximised and the most noble metal tends to occupy the core of the metal-atom polyhedron. However, in the absence of site preference dictated by the geometry of the cluster framework, M/M′ substitutional disorder has been observed, for example, in the series of clusters of the formula $[H_{4-n}Ni_{12-x}Pt_x(CO)_{21}]^{n-}$ ($n = 2$–4; $x \geq 3$)[12–15] and $[Ni_{10}(Ni_{6-x}Pt_x)Pt_8(CO)_{30}]^{4-}$ ($x = 2$).[7] Even a non-stoichiometric species, for example, the trimetallic $[Ni_{20}(Ni_{6-x}Pd_x)Pd_6Au_6(CO)_{48}]^{6-}$ ($x = 2.1$–5.5),[16] has been isolated.

The present work originates from the recognition that high-nuclearity metal carbonyl clusters often behave as nanosized molecular capacitors,[6,17] as well as the observation that their electronic and chemical behaviour are modu-

[a] Dr. C. Femoni, Prof. M. C. Iapalucci, Prof. G. Longoni, Dr. P. H. Svensson
Dipartimento di Chimica Fisica ed Inorganica
viale Risorgimento 4, 40136 Bologna (Italy)
Fax: (+39) 51-2093690
E-mail: longoni@ms.fci.unibo.it.

[b] Dr. P. H. Svensson
Present address: AstraZeneca R&D Sodertalje Solid State Analysis
151 85 Sodertalje (Sweden)

[c] Prof. P. Zanello, Dr. F. Fabrizi de Biani
Dipartimento di Chimica
via A. Moro, 53100 Siena (Italy)

DOI: 10.1002/chem.200305210

lated by the metal composition, for example $[Rh_{14-x}Ni_x(CO)_{25}]^{n-}$ ($x = 0, 1, 2, 5$).[18]

As part of our efforts to develop more efficient molecular capacitors, we wished to test the effect of substituting the internal Pt atoms of $[Ni_{38}Pt_6(CO)_{48}]^{6-}$ with Pd atoms, as well as the partial exchange of surface Ni with congener Pd or Pt atoms. We report here the synthesis, structure and chemical behaviour of two new ν_3-octahedral bimetallic clusters of $[Ni_{35}Pt_9(CO)_{48}]^{6-}$ and $[Ni_{36}Pd_8(CO)_{48}]^{6-}$ stoichiometry. The latter establishes a first structural similarity between the carbonylated Ni–Pd and Ni–Pt clusters.

Results and Discussion

Synthesis and chemical characterisation of $[Ni_{35}Pt_9(CO)_{48}]^{6-}$ and $[Ni_{36}Pd_8(CO)_{48}]^{6-}$: Several years ago, we reported the synthesis of $[H_{6-n}Ni_{38}Pt_6(CO)_{48}]^{n-}$ ($n = 4, 5, 6$) clusters by reaction of $[Ni_6(CO)_{12}]^{2-}$ with Pt^{II} reagents in acetonitrile, according to the formal stoichiometry of Equation (1).[5]

$$7\,[Ni_6(CO)_{12}]^{2-} + 6\,[PtCl_4]^{2-} \rightarrow [Ni_{38}Pt_6(CO)_{48}]^{6-} + 2\,[Ni(CO)_4] + 2\,Ni^{2+} + 24\,Cl^- + 28\,CO \quad (1)$$

The formation of hydride derivatives was attributed to protonation of the resulting hexaanion by any M^{II} aqua complex produced in the reaction solution by the presence of humidity. More recently, a related reaction involving 1.5–2 moles of Pt^{II} reagents per mole of $[Ni_6(CO)_{12}]^{2-}$ afforded the $[Ni_{24}Pt_{14}(CO)_{44}]^{4-}$ derivative.[7] The present choice of molar ratios midway between those previously adopted for the synthesis of $[HNi_{38}Pt_6(CO)_{48}]^{5-}$ and $[Ni_{24}Pt_{14}(CO)_{44}]^{4-}$ affords yet another Ni–Pt species, namely, $[Ni_{35}Pt_9(CO)_{48}]^{6-}$. This is conveniently obtained by reaction in ethyl acetate or THF of $[NBu_4]_2[Ni_6(CO)_{12}]$ with $[Pt(SEt_2)_2Cl_2]$ in a 1:1.1 molar ratio. The resulting brown precipitate is slightly soluble in THF and fairly soluble in acetone. As shown by IR and ESI-MS monitoring, both solutions contain a mixture of $[Ni_{35}Pt_9(CO)_{48}]^{6-}$ and $[HNi_{35}Pt_9(CO)_{48}]^{5-}$. A THF solution affords well-shaped crystals of $[NBu_4]_6[Ni_{35}Pt_9(CO)_{48}]\cdot 6\,THF$ upon standing. Crystals are obtained from the THF mother liquor and the acetone extract only after deprotonation of $[HNi_{35}Pt_9(CO)_{48}]^{5-}$ to $[Ni_{35}Pt_9(CO)_{48}]^{6-}$ with sodium methoxide and layering with hexane and isopropyl alcohol, respectively. All crystalline samples show similar ESI-MS profiles and Ni/Pt ratios of ≈ 3.9, in close agreement with the $[Ni_{35}Pt_9(CO)_{48}]^{6-}$ composition later established by X ray structural analysis. The overall yield is $\approx 60\,\%$ (based on Pt).

The $[Ni_{35}Pt_9(CO)_{48}]^{6-}$ hexaanion is partially and quantitatively protonated by water and diluted solutions of acids in THF [Eq. (2)], respectively. The resulting $[HNi_{35}Pt_9(CO)_{48}]^{5-}$ pentaanion has been isolated by precipitation with water. Further protonation to $[H_2Ni_{35}Pt_9(CO)_{48}]^{4-}$ only occurs to a small extent, even upon addition of excess acid and is accompanied by decomposition.

$$\underset{\nu_{CO}\text{ in THF}}{[Ni_{35}Pt_9(CO)_{48}]^{6-}} \underset{CH_3CN}{\overset{H^+,THF}{\rightleftharpoons}} \underset{\nu_{CO}\text{ in THF}}{[HNi_{35}Pt_9(CO)_{48}]^{5-}} \underset{CH_3CN}{\overset{H^+,THF}{\rightleftharpoons}} \underset{\nu_{CO}\text{ in THF}}{[H_2Ni_{35}Pt_9(CO)_{48}]^{4-}}$$

2001 (s) 2011 (s) 2023 (s)

1861 (m) 1873 (m) 1885 (m)

(2)

This represents a first difference in the reactivity between the related $[Ni_{35}Pt_9(CO)_{48}]^{6-}$ and $[Ni_{38}Pt_6(CO)_{48}]^{6-}$ clusters. The latter, indeed, has been reversibly protonated up to the $[H_3Ni_{38}Pt_6(CO)_{48}]^{3-}$ ion. Furthermore, the tetra- and pentaanions have been isolated in the solid state and partially or fully characterised by X-ray diffraction.[5,6] The $[H_{6-n}Ni_{35}Pt_9(CO)_{48}]^{n-}$ ($n = 6, 5$) derivatives display IR carbonyl absorptions slightly, but noticeably, shifted to higher wavenumbers with respect to their corresponding $[H_{6-n}Ni_{38}Pt_6(CO)_{48}]^{n-}$ counterparts. This is in agreement with a greater Pt content, which implies the presence of surface Pt atoms and, consequently, Pt–CO interactions. As for $[H_{6-n}Ni_{38}Pt_6(CO)_{48}]^{n-}$, the hydride nature of $[HNi_{35}Pt_9(CO)_{48}]^{5-}$ could not be directly proven by ^1H NMR spectroscopy. The purported presence of a hydride atom is, however, supported by circumstantial evidence, such as the occurrence of a protonation–deprotonation equilibrium in ionising solvents and distinctive electrochemical behaviour (see below).

A further significant difference between $[Ni_{38}Pt_6(CO)_{48}]^{6-}$ and $[Ni_{35}Pt_9(CO)_{48}]^{6-}$ is represented by the decreased stability of the redox products of the latter. Indeed, chemical reduction of $[Ni_{35}Pt_9(CO)_{48}]^{6-}$ with sodium naphthalenide reversibly affords $[Ni_{35}Pt_9(CO)_{48}]^{7-}$ (ν_{CO} in THF at 1985 (s) and 1845 (m) cm^{-1}) and $[Ni_{35}Pt_9(CO)_{48}]^{8-}$ (ν_{CO} in THF at 1975 (s) and 1831 (m) cm^{-1}) in sequence. These two new anions quantitatively regenerate the parent $[Ni_{35}Pt_9(CO)_{48}]^{6-}$ hexaanion upon oxidation with tropylium tetrafluoroborate. As inferable from IR, $[Ni_{35}Pt_9(CO)_{48}]^{7-}$ is stable in solution for several hours, while $[Ni_{35}Pt_9(CO)_{48}]^{8-}$ releases decomposition products upon standing for a few hours. Oxidation of $[Ni_{35}Pt_9(CO)_{48}]^{6-}$ with tropylium tetrafluoroborate in acetonitrile initially gives rise to a species showing its maximum absorptions at 2013 and 1864 cm^{-1}, tentatively formulated as $[Ni_{35}Pt_9(CO)_{48}]^{5-}$. However, before completion of the oxidation, a further shift of the absorption frequencies up to 2030 and 1878 cm^{-1} takes place. Subsequent reduction of the latter species with sodium naphthalenide in THF does not re-afford the parent $[Ni_{35}Pt_9(CO)_{48}]^{6-}$ compound.

The reaction of $[NBu_4]_2[Ni_6(CO)_{12}]$ with $[Pd(SEt_2)_2Cl_2]$ has little or no resemblance to the corresponding reaction of $[NBu_4]_2[Ni_6(CO)_{12}]$ with $[Pt(SEt_2)_2Cl_2]$ both in THF and in ethyl acetate. As previously reported, the complete disappearance of the IR carbonyl absorptions of $[Ni_6(CO)_{12}]^{2-}$ from the reaction solution requires the addition of more than two moles of $[Pd(SEt_2)_2Cl_2]$. Work-up of the resulting brown suspension has so far allowed isolation of Pd-rich $[Ni_{16}Pd_{16}(CO)_{40}]^{4-}$,[2] $[Ni_{26}Pd_{20}(CO)_{54}]^{6-}$[2] and $[Ni_{22}Pd_{20}(CO)_{48}]^{6-}$ species. The latter probably corresponds to the species previously isolated by Dahl and co-workers.[19] In the attempt to isolate a $[Ni_{44-x}Pd_x(CO)_{48}]^{6-}$ species, related to $[Ni_{38}Pt_6(CO)_{48}]^{6-}$ or $[Ni_{35}Pt_9(CO)_{48}]^{6-}$, we set up a

series of reactions in THF between $[NBu_4]_2[Ni_6(CO)_{12}]$ and $[Pd(SEt_2)_2Cl_2]$ in 1:1.1–1.3 molar ratios, to keep unreacted $[Ni_6(CO)_{12}]^{2-}$ dianion still present in the solution at the end of the reaction. The resulting brown suspension was stirred for several days and then worked-up as follows: the residual $[Ni_6(CO)_{12}]^{2-}$ and $[Ni_{22}Pd_{20}(CO)_{48}]^{6-}$ salts were eliminated by extraction in THF. The brown residue was extracted with acetone and partially precipitated with isopropyl alcohol to give crude $[Ni_{16}Pd_{16}(CO)_{40}]^{4-}$. The mother liquor was evaporated to dryness, and the residue was crystallised from acetone/hexane. An X-ray diffraction study of the resulting crystals allowed us to establish the composition as $[NBu_4]_{12}[Ni_{30}(Ni_{8-x}Pd_x)Pd_6(CO)_{48}][Ni_{30}(Ni_{8-x'}Pd_{x'})Pd_6(CO)_{48}]\cdot 6(CH_3)_2CO\cdot C_6H_{14}$ (x and $x' = 2$). The yields are very poor (≈5–10% based on Pd) because of the limited differential solubility of $[Ni_{22}Pd_{20}(CO)_{48}]^{6-}$, $[Ni_{16}Pd_{16}(CO)_{40}]^{4-}$ and $[Ni_{36}Pd_8(CO)_{48}]^{6-}$ as their tetrabutylammonium salts. Elemental analysis of the crystals gave a Ni/Pd ratio of ≈4.5, as expected for the above composition. The acetone solution of the salt shows an IR pattern very similar to that displayed by related bimetallic Ni-Pt hexaanions [Eq. (3)].

$$[Ni_{36}Pd_8(CO)_{48}]^{6-} \underset{DMSO}{\overset{H^+,MeCN}{\rightleftharpoons}} [HNi_{36}Pd_8(CO)_{48}]^{5-} \underset{MeCN}{\overset{H^+,Me_2CO}{\rightleftharpoons}}$$

		$[H_2Ni_{36}Pd_8(CO)_{48}]^{4-}$
ν_{CO} in MeCN	ν_{CO} in MeCN	ν_{CO} in Me_2CO
1990 (s)	2005 (s)	2015 (s)
1848 (m)	1857 (m)	1865 (m)

(3)

As for $[Ni_{35}Pt_9(CO)_{48}]^{6-}$, the $[HNi_{36}Pd_8(CO)_{48}]^{5-}$ pentaanion is readily obtained by protonation of the parent hexaanion with a stoichiometric amount of sulfuric acid diluted in CH_3CN solution [Eq. (3)] and has been isolated in the solid state by precipitating with water. In contrast to $[HNi_{35}Pt_9(CO)_{48}]^{5-}$, further protonation in acetone of $[HNi_{36}Pd_8(CO)_{48}]^{5-}$ quantitatively affords the $[H_2Ni_{36}Pd_8(CO)_{48}]^{4-}$ ion [Eq. (3)], which was isolated as described above. The hydride nature of $[H_{6-n}Ni_{36}Pd_8(CO)_{48}]^{n-}$ ($n = 5, 4$) could not be directly proven by ^1H NMR spectroscopy. The purported presence of hydride atoms is suggested by circumstantial evidence, such as their deprotonation equilibria in acetonitrile and DMSO, respectively.

The above suggestion is also substantiated by the chemical oxidation of $[Ni_{36}Pd_8(CO)_{48}]^{6-}$ with tropylium tetrafluoroborate. The resulting yet uncharacterised product did not regenerate the parent compound upon reduction.

Electrochemical behaviour of $[Ni_{35}Pt_9(CO)_{48}]^{6-}$: The (square-wave) voltammetric profiles of a mixture of $[Ni_{35}Pt_9(CO)_{48}]^{6-}$ and $[HNi_{35}Pt_9(CO)_{48}]^{5-}$ in DMF just after its dissolution and after 90 min are shown in Figure 1. Their comparison points out that the initially present starred peaks progressively tend to disappear on standing. According to the chemistry reported in Equation (2), the starred peaks are attributed to redox processes of $[HNi_{35}Pt_9(CO)_{48}]^{5-}$. This behaviour provides further circumstantial evidence of the hydride nature of the latter. It is also deducible that the most anodic process is greatly overlapped by the oxidation of the residual hydride complex.

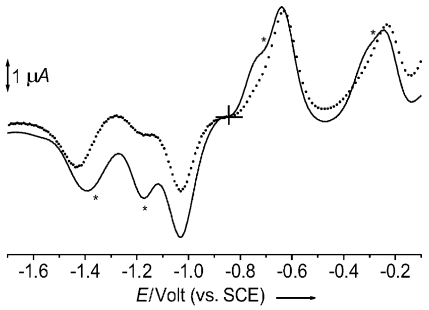

Figure 1. Osteryoung voltammetric profiles of an approximately 1:1 mixture of $[NBu_4]_6[Ni_{35}Pt_9(CO)_{48}]$ and $[NBu_4]_5[HNi_{35}Pt_9(CO)_{48}]$ (7×10^{-4} mol dm^{-3}) recorded under the following conditions: a) immediately after its dissolution in DMF solution (——), b) after 90 min (-----). Scan rate 0.1 V s^{-1}, supporting electrolyte $[NBu_4][PF_6]$ (0.2 mol dm^{-3}), gold working electrode.

The cyclic voltammetric profile of the mixture of $[Ni_{35}Pt_9(CO)_{48}]^{6-}$ and $[HNi_{35}Pt_9(CO)_{48}]^{5-}$ after 90 min standing in DMF solution is shown in Figure 2. The

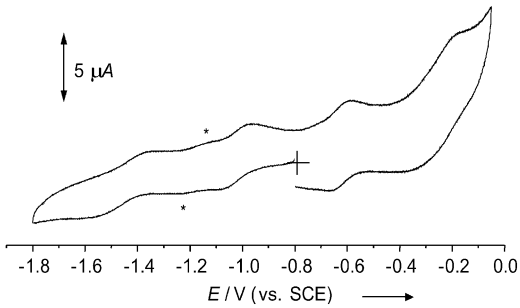

Figure 2. Cyclic voltammetric profile of an approximately 1:1 mixture of $[NBu_4]_6[Ni_{35}Pt_9(CO)_{48}]$ and $[NBu_4]_5[HNi_{35}Pt_9(CO)_{48}]$ (7×10^{-4} mol dm^{-3}) in DMF after standing for 90 min. Scan rate 0.2 V s^{-1}, supporting electrolyte $[NBu_4][PF_6]$ (0.2 mol dm^{-3}), gold electrode.

$[Ni_{35}Pt_9(CO)_{48}]^{6-}$ ion undergoes a first one-electron reduction and a first one-electron oxidation, both possessing features of chemical ($i_{p(return)}/i_{p(forward)} = 1$) and electrochemical ($\Delta E_p \approx 60$ mV) reversibility in cyclic voltammetry. Both are followed in turn by a second quasi-reversible one-electron reduction and an almost irreversible multielectron oxidation, respectively. The low current density made it impossible to experimentally measure the number of electrons involved in each step by controlled potential coulometry. The starred peak in Figure 2 is clearly attributable to minor amounts of $[HNi_{35}Pt_9(CO)_{48}]^{5-}$.

Table 1 gives the electrode potentials for the above-mentioned redox processes of $[Ni_{35}Pt_9(CO)_{48}]^{6-}$ and its hydride congener $[HNi_{35}Pt_9(CO)_{48}]^{5-}$, also in comparison with the series $[H_{6-n}Ni_{38}Pt_6(CO)_{48}]^{n-}$ ($n = 6, 5$).[6] It seems evident that substitution of Ni with Pt atoms in $[H_{6-n}Ni_{38}Pt_6(CO)_{48}]^{n-}$ ($n = 6, 5$) significantly reduces the redox flexibility of the resulting $[H_{6-n}Ni_{35}Pt_9(CO)_{48}]^{n-}$ complexes.

Table 1. Formal electrode potentials [V, versus SCE] measured by Osteryoung square-wave voltammetry for the redox processes exhibited by $[Ni_{35}Pt_9(CO)_{48}]^{6-}$ and $[Ni_{38}Pt_6(CO)_{48}]^{6-}$[6] in DMF solution.

Complex	$E^{\circ\prime}_{3-/4-}$	$E^{\circ\prime}_{4-/5-}$	$E^{\circ\prime}_{5-/6-}$	$E^{\circ\prime}_{6-/7-}$	$E^{\circ\prime}_{7-/8-}$	$E^{\circ\prime}_{8-/9-}$	$E^{\circ\prime}_{9-/10-}$
$[Ni_{35}Pt_9(CO)_{48}]^{6-}$		−0.23[a]	−0.63	−1.03	−1.43		
$[HNi_{35}Pt_9(CO)_{48}]^{5-}$	−0.30	−0.73	−1.17	−1.38			
$[Ni_{38}Pt_6(CO)_{48}]^{6-}$			−0.62	−0.97	−1.29	−1.54	−1.75
$[HNi_{38}Pt_6(CO)_{48}]^{5-}$		−0.61	−0.98	−1.28	−1.55		

[a] Assumed to be a one-electron process; see text.

ESI mass spectrometry studies of $[NBu_4]_6[Ni_{35}Pt_9(CO)_{48}]$ and $[NBu_4]_6[Ni_{36}Pd_8(CO)_{48}]$: The enormous potential of ESI-MS (electrospray ionisation mass spectrometry) in studying sparingly volatile neutral organometallic compounds[20] and clusters,[21] as well as nonvolatile cluster salts, has widely been recognised.[22–24] To our knowledge, the largest cluster so far studied by ESI-MS is the $[Os_{20}(CO)_{40}]^{2-}$ dianion.[25]

A typical ESI-MS spectrum of a crystalline $[NBu_4]_6[Ni_{24}(Ni_{14-x}Pt_x)Pt_6(CO)_{48}]$ sample roughly consists of two sets of signals approximately located in the regions m/z 3218–2660 and 1990–1500. All multiplets falling in these regions appear to originate from a $[NBu_4]_6[Ni_{35}Pt_9(CO)_{48}]$ salt. The multiplets in the m/z 3218–2660 range are all interpretable as arising from the isotopic composition of two sets of dianions of general formula $\{[NBu_4]_m[Ni_{35}Pt_9(CO)_n]\}^{2-}$ (m = 1–5; n = 47 or 46) and $\{[NBu_4]_m[Ni_{33}Pt_9(CO)_n]\}^{2-}$ (m = 2–6; n = 45–47). The multiplets in the m/z 1990–1500 range can be attributed to a wider set of trianions, all of them generated by the isotopic composition of the following species: $\{[NBu_4]_m[Ni_{35}Pt_9(CO)_{46}]\}^{3-}$ (m = 3, 2), $\{[NBu_4]_m[Ni_{34}Pt_9(CO)_n]\}^{3-}$ (m = 4, 3, 1; n = 47 or 46), $\{[NBu_4]_m[Ni_{33}Pt_9(CO)_n]\}^{3-}$ (m = 3, 2; n = 46 or 44 or 43), $\{[NBu_4][Ni_{32}Pt_9(CO)_{43}]\}^{3-}$, $[Ni_{30}Pt_9(CO)_{46}]^{3-}$, $\{[NBu_4]_m[Ni_{29}Pt_9(CO)_n]\}^{3-}$ (m = 2, 1, 0; n = 44 or 43). A comparison between the most intense peak of each multiplet and the calculated average molecular weight is reported in Table 2. No spurious peak, originating from Ni–Pt carbonylated species other than $[Ni_{35}Pt_9(CO)_{48}]^{6-}$ could be identified. It is, therefore, concluded that the $[Ni_{35}Pt_9(CO)_{48}]^{6-}$ salts mainly undergo cation, CO and/or $[Ni(CO)_x]$ elimination as preferential fragmentation processes. The final $[Ni_{29}Pt_9(CO)_{44}]^{n-}$ ion is probably related to the known truncated octahedral $[Ni_{24}Pt_{14}(CO)_{44}]^{4-}$[7] cluster. Moreover, since all observed multiplets can be attributed to ions all featuring nine Pt atoms, this rules out the presence of compositionally different $[Ni_{24}(Ni_{14-x}Pt_x)Pt_6(CO)_{48}]^{6-}$ ($14 \geq x \geq 0$) congener ions with a distribution giving rise to an average x value of 3.

Related investigations aimed at investigating ESI-MS signals of $[NBu_4]_n[H_{6-n}Ni_{36}Pd_8(CO)_{48}]$ (n = 4–6) salts met no success on account of complete fragmentation into meaningless low molecular-weight species.

X-ray structure of $[NBu_4]_6[Ni_{35}Pt_9(CO)_{48}]\cdot 6$THF showing the presence of a substitutionally Ni/Pt disordered $[Ni_{24}(Ni_{14-x}Pt_x)Pt_6(CO)_{48}]^{6-}$ ion: The asymmetric unit of the $[NBu_4]_6[Ni_{35}Pt_9(CO)_{48}]\cdot 6$THF salt contains one half anion located on a crystallographic centre of symmetry, three $[NBu_4]^+$ ions and three THF molecules. The overall structure of the $[Ni_{35}Pt_9(CO)_{48}]^{6-}$ ion is very similar to that previously ascertained for the $[HNi_{38}Pt_6(CO)_{48}]^{5-}$ ion and has been refined as a substitutional Ni/Pt disordered $[Ni_{24}(Ni_{14-x}Pt_x)Pt_6(CO)_{48}]^{6-}$ (x = 3; see the Experimental Section) ion. As shown in Figure 3a, the metal framework consists of a $[Ni_{24}(Ni_{14-x}Pt_x)]$ ν_3 octahedron encapsulating a Pt_6 octahedron. In Figure 3 (as well as Figure 4) Ni and Pt sites are shown in yellow and blue, respectively, while disordered Ni/Pt sites are shown in magenta (Ni/Pt = 0.57/0.43) and green (Ni/Pt = 0.93/0.07). A different view of the metal framework of the above cluster ion is given in Figure 3b. It shows the metal atom aggregation as four close-packed layers giving rise to a fragment with a cubic close packing structure (the one adopted by both metals in the bulk). This second view shows that two opposite faces of the ν_3 octahedron (top and bottom faces of Figure 3b) differentiate from the other six as they are uniquely composed of nickel atoms, while all sites but four of the two internal layers are more or less involved in Pt segregation. This could suggest a sandwich segregation of Ni and Pt along the idealised C_3 axis perpendicular to the top face. A Pt-Ni-Pt oscillatory layer-dependent segregation has been observed for (111) surfaces

Table 2. Ions found in the ESI mass spectrum of $[Ni_{35}Pt_9(CO)_{48}]^{6-}$.

m/z	Rel. int.	Ion	MW/z
3218	10	$\{[N(C_4H_9)_4]_6[Ni_{33}Pt_9(CO)_{46}]\}^{2-}$	3217.9
3165	10	$\{[N(C_4H_9)_4]_5[Ni_{35}Pt_9(CO)_{47}]\}^{2-}$	3169.4
3108	14	$\{[N(C_4H_9)_4]_5[Ni_{33}Pt_9(CO)_{47}]\}^{2-}$	3110.6
3098	20	$\{[N(C_4H_9)_4]_5[Ni_{33}Pt_9(CO)_{46}]\}^{2-}$	3096.7
3044	20	$\{[N(C_4H_9)_4]_4[Ni_{35}Pt_9(CO)_{47}]\}^{2-}$	3048.2
2972	17	$\{[N(C_4H_9)_4]_4[Ni_{33}Pt_9(CO)_{46}]\}^{2-}$	2975.5
2923	30	$\{[N(C_4H_9)_4]_3[Ni_{35}Pt_9(CO)_{47}]\}^{2-}$	2926.9
2908	28	$\{[N(C_4H_9)_4]_3[Ni_{35}Pt_9(CO)_{46}]\}^{2-}$	2912.9
2853	26	$\{[N(C_4H_9)_4]_3[Ni_{33}Pt_9(CO)_{46}]\}^{2-}$	2854.2
2784	21	$\{[N(C_4H_9)_4]_2[Ni_{35}Pt_9(CO)_{45}]\}^{2-}$	2777.7
2717	17	$\{[N(C_4H_9)_4]_2[Ni_{33}Pt_9(CO)_{45}]\}^{2-}$	2718.9
2670	10	$\{[N(C_4H_9)_4][Ni_{35}Pt_9(CO)_{46}]\}^{2-}$	2670.5
1987	20	$\{[N(C_4H_9)_4]_4[Ni_{34}Pt_9(CO)_{44}]\}^{3-}$	1984.5
1942	23	$\{[N(C_4H_9)_4]_3[Ni_{35}Pt_9(CO)_{46}]\}^{3-}$	1941.9
1932	35	$\{[N(C_4H_9)_4]_3[Ni_{34}Pt_9(CO)_{47}]\}^{3-}$	1931.7
1896	38	$\{[N(C_4H_9)_4]_3[Ni_{33}Pt_9(CO)_{45}]\}^{3-}$	1893.5
1860	60	$\{[N(C_4H_9)_4]_2[Ni_{35}Pt_9(CO)_{46}]\}^{3-}$	1861.1
1813	86	$\{[N(C_4H_9)_4]_2[Ni_{34}Pt_9(CO)_{43}]\}^{3-}$	1813.5
1769	100	$\{[N(C_4H_9)_4][Ni_{34}Pt_9(CO)_{47}]\}^{3-}$	1770.1
1725	85	$\{[N(C_4H_9)_4]_2[Ni_{29}Pt_9(CO)_{44}]\}^{3-}$	1725.1
1722	78	$\{[N(C_4H_9)_4][Ni_{33}Pt_9(CO)_{44}]\}^{3-}$	1722.5
1689	71	$\{[N(C_4H_9)_4][Ni_{32}Pt_9(CO)_{43}]\}^{3-}$	1693.6
1644	47	$\{[N(C_4H_9)_4][Ni_{29}Pt_9(CO)_{44}]\}^{3-}$	1644.2
1635	30	$\{[N(C_4H_9)_4][Ni_{29}Pt_9(CO)_{43}]\}^{3-}$	1634.9
1599	25	$\{[Ni_{30}Pt_9(CO)_{46}]\}^{3-}$	1601.6
1561	18	$\{[Ni_{29}Pt_9(CO)_{44}]\}^{3-}$	1563.4

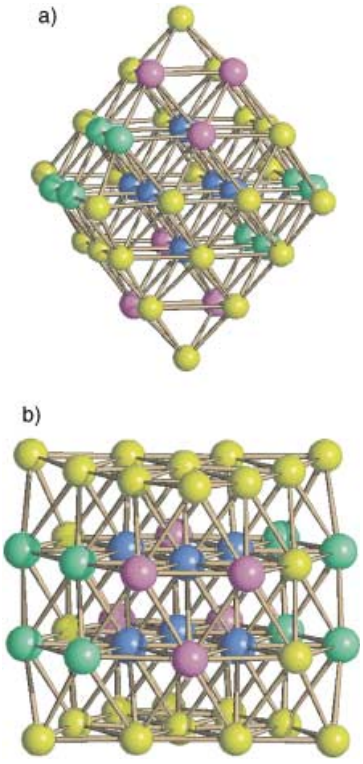

Figure 3. Two views of the substitutionally Ni/Pt disordered metal frame of $[Ni_{24}(Ni_{14-x}Pt_x)Pt_6(CO)_{48}]^{6-}$ ($x = 3$), (Ni = yellow, Pt = blue, Ni/Pt (≈57:43) magenta, Ni/Pt (≈93:7) green).

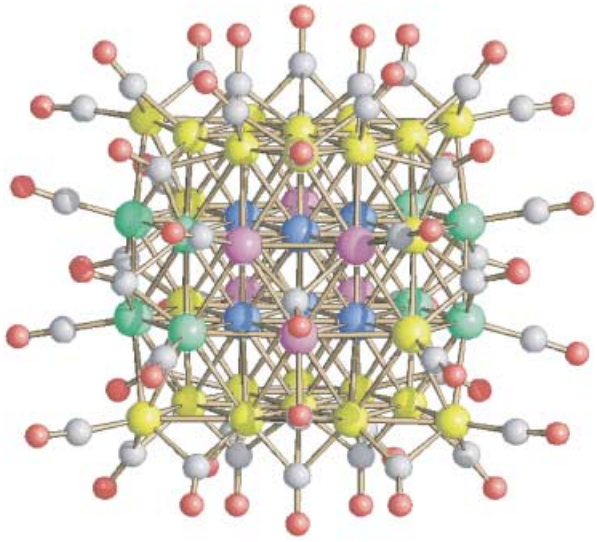

Figure 4. The whole structure of the $[Ni_{24}(Ni_{14-x}Pt_x)Pt_6(CO)_{48}]^{6-}$ ion ($x = 3$; colours as in Figure 3).

of Ni–Pt alloys,[26] whereas a reversed Ni-Pt-Ni oscillatory enrichment has been found for the three uppermost (110) layers of the same Ni-Pt bulk alloys by LEED experiments.[27] The interpretations offered for the above surface-sandwich segregation[28,29] do not apply to the present case.

The whole structure of the $[Ni_{24}(Ni_{14-x}Pt_x)Pt_6(CO)_{48}]^{6-}$ ion is shown in Figure 4, and the average values and the ranges of most significant interatomic distances are collected in Table 3. The carbonyl groups may be roughly classified as terminal (18), edge-bridging (12) and face-bridging (18) ligands. However, some edge- and face-bridging carbonyl groups are so unsymmetrical that they could be alternatively described as terminal ligands that lean towards one or two neighbouring metal atoms, or as edge-bridging ligands that lean towards a third metal. This is particularly relevant for face-bridging ligands that consequently show the widest range of M–C interactions. In detail, each Ni vertex of the ν_3 octahedron is bound to one terminal and two edge-bridging ligands. The atoms centring the eight ν_3-triangular faces of the octahedron are divided into three sets: a pair of metal atoms, centring the top and bottom faces of the ν_3 octahedron, as shown in Figure 3b, is bound to two face-bridging carbonyl groups and loosely interacts with a third. The three are coordinated to alternate triangular faces sharing a common Ni centre. Of the six atoms centring the remaining six faces, four are disordered Ni/Pt sites displaying either 0.43 (two sites) or 0.07 (two sites) Pt fractions and two are Ni atoms. All them are roughly bound to two face-bridging carbonyl groups capping two opposite triangular faces. However, the two Ni and the two Ni/Pt sites featuring a 0.07 Pt fraction are bonded to two symmetrical face-bridging carbonyl groups, whereas for the two Ni/Pt featuring a 0.43 Pt fraction, one of the two face-bridging carbonyls is so unsymmetrical that it could be alternatively classified as a terminal ligand leaning towards a pair of Ni atoms.

The twelve pairs of edge-sites of the ν_3 octahedron are also divided in two sets: the six pairs of Ni atoms belonging to the top and bottom face are bound to one edge and two face-bridging ligands. The remaining six pairs of metal sites belonging to the two inner layers are bound to one face-bridging ligand and one terminal ligand. Of these, four pairs are disordered Ni/Pt sites.

Table 3. Average M–M bond lengths and corresponding individual ranges [Å] for $[Ni_{24}(Ni_{14-x}Pt_x)Pt_6(CO)_{48}]^{6-}$ ($x = 3$), **A**, $[Ni_{30}(Ni_{8-x}Pd_x)Pd_6(CO)_{48}]^{6-}$ ($x = 2$, first ion), **B**, and $[Ni_{30}(Ni_{8-x}Pd_x)Pd_6(CO)_{48}]^{6-}$ ($x = 2$, second ion), **C**.[a]

	A		**B**		**C**	
	Av	Range	Av	Range	Av	Range
M–M	2.728	2.717(1)–2.740(1)	2.693	2.680(1)–2.706(2)	2.705	2.693(1)–2.719(1)
M–Ni	2.658	2.600(1)–2.735(1)	2.568	2.525(1)–2.615(1)	2.576	2.525 (1)–2.626(1)
Ni–Ni	2.566	2.430(3)–2.767(3)	2.568	2.400(2)–2.812(2)	2.572	2.406(2)–2.839(2)
Ni/M–M	2.651	2.578(2)–2.736(1)	2.719	2.642(1)–2.859(2)	2.719	2.651(1)–2.860(2)
Ni/M–Ni	2.647	2.592(2)–2.733(2)	2.592	2.511(1)–2.634(1)	2.599	2.514(1)–2.643(1)
Ni/M–Ni/M	2.667	2.614(2)–2.731(1)	–	–	–	–
Ni–C_t or Ni/M–C_t	1.75	1.69(1)–1.79(1)	1.77	1.76(1)–1.78(1)	1.77	1.75(1)–1.78(1)
Ni–C_{eb} or Ni/M–C_{eb}	1.90	1.82(2)–1.99(2)	1.90	1.85(1)–1.95(1)	1.90	1.84(1)–1.95(1)
Ni–C_{fb} or Ni/M–C_{fb}	1.96	1.65(7)–2.12(2)	1.99	1.87(1)–2.16(1)	2.00	1.88(1)–2.18(1)

[a] t = terminal, eb = edge-bridging, fb = face-bridging

X-ray structure of $[NBu_4]_{12}[Ni_{30}(Ni_{8-x}Pd_x)Pd_6(CO)_{48}][Ni_{30}(Ni_{8-x'}Pd_{x'})Pd_6(CO)_{48}]\cdot 6(CH_3)_2CO\cdot C_6H_{14}$ (x and $x' = 2$): The asymmetric unit of the $[NBu_4]_{12}[Ni_{30}(Ni_{8-x}Pd_x)Pd_6(CO)_{48}][Ni_{30}(Ni_{8-x'}Pd_{x'})Pd_6(CO)_{48}]\cdot 6(CH_3)_2CO\cdot C_6H_{14}$ (x and $x' = 2$) salt contains two independent half-anions, six $[NBu_4]^+$ ions, three acetone molecules and a half molecule of *n*-hexane. The overall structures of the two independent $[Ni_{36}Pd_8(CO)_{48}]^{6-}$ ions are very similar and the two ions only slightly differ in the relative Pd fraction found in each substitutionally Ni/Pd disordered site. That is the reason to keep the x and x' notation. Both ions consist of a $[Ni_{30}(Ni_{8-x}Pd_x)]$ ν_3 octahedron encapsulating a Pd_6 octahedron. For both ions, the disordered sites are those centring the eight triangular faces of the ν_3-octahedral moiety. As a consequence, only a pictorial representation of the metal framework of the first ion is given in Figure 5, where Ni and Pd

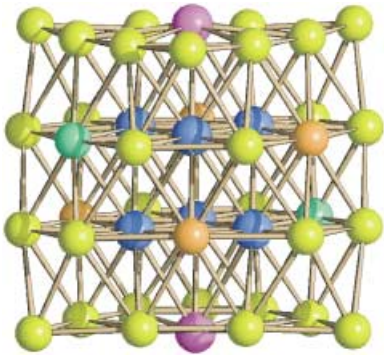

Figure 5. The substitutionally Ni/Pd disordered metal frame of $[Ni_{30}(Ni_{8-x}Pd_x)Pd_6(CO)_{48}]^{6-}$ ($x = 2$, first ion), (Ni = yellow, Pd = blue, Ni/Pd ($\approx$37:63) magenta, Ni/Pd ($\approx$83:17) green), Ni/Pd ($\approx$90:10) orange.

sites are shown in yellow and blue, whereas disordered Ni/Pd sites are shown in different colours roughly according with their Pd fractions. The refined Pd fraction of four surface sites (orange spheres in Figures 5 and 6) of each ion is very small (0.05–0.1). Nevertheless, we decided to take it into account after refining other alternative models (see the Experimental Section).

The whole structures of the two $[Ni_{30}(Ni_{8-x}Pd_x)Pd_6(CO)_{48}]^{6-}$ ions are also practically identical; only that of the first ion is reported in Figure 6. The most significant interatomic distances of both ions are collected in Table 3. The overall distribution and stereochemistry of the CO groups is almost coincident with that just described for $[Ni_{35}Pt_9(CO)_{48}]^{6-}$. However, the underlying metal distribution is different: each Ni vertex of the ν_3 octahedron is bound to one terminal and two edge-bridging ligands. The atoms centring the eight ν_3-triangular faces of the octahedron are divided in two sets. A pair of metal atoms, centring two opposite faces of the ν_3 octahedron, is bound to three symmetrical face-bridging carbonyl groups coordinated to three alternate triangular faces. These sites (magenta spheres) are the Ni/Pd disordered sites with the highest Pd fraction (0.63 and 0.72 in the two independent ions, respectively). The atoms centring the remaining six faces are all disordered Ni/Pd sites displaying Pd fractions (values in parenthesis refer to the second ion) of 0.17 (0.18), 0.1 (0.05) and 0.1 (0.05). All of them are bound to two face-bridging carbonyl groups coordinated to two opposite triangular faces. The 24 edge sites are Ni atoms and may be divided in two sets: those belonging to the top and bottom face are bound to one edge- and two face-bridging CO ligands. Those belonging to the interlayer edges are bound to one terminal and one face-bridging ligand.

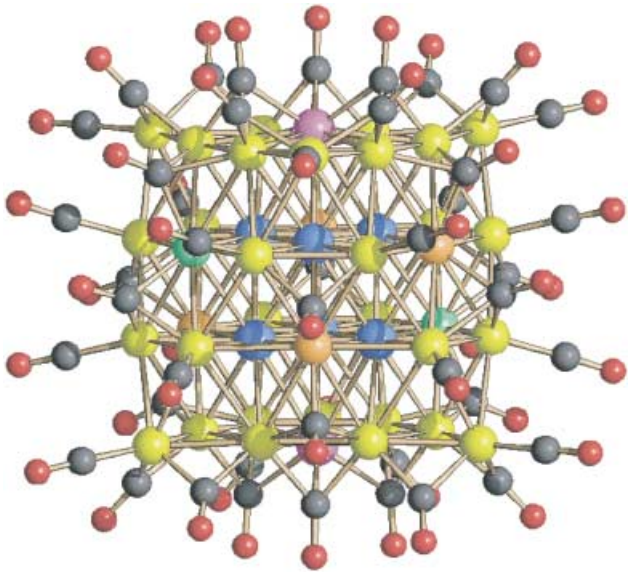

Figure 6. The whole structure of the $[Ni_{30}(Ni_{8-x}Pd_x)Pd_6(CO)_{48}]^{6-}$ ion ($x = 2$, first ion; colours as in Figure 5).

Analysis of the substitutional Ni/Pt and Ni/Pd disorder of $[NBu_4]_6[Ni_{24}(Ni_{14-x}Pt_x)Pt_6(CO)_{48}]\cdot 6THF$ ($x = 3$) and $[NBu_4]_{12}[Ni_{30}(Ni_{8-x}Pd_x)Pd_6(CO)_{48}][Ni_{30}(Ni_{8-x'}Pd_{x'})Pd_6(CO)_{48}]\cdot 6(CH_3)_2CO\cdot C_6H_{14}$ (x and $x' = 2$): The observed substitutional Ni/Pt and Ni/Pd disorder of $[Ni_{24}(Ni_{14-x}Pt_x)Pt_6(CO)_{48}]^{6-}$ ($x = 3$) and $[Ni_{30}(Ni_{8-x}Pd_x)Pd_6(CO)_{48}]$ ($x = 2$) could have several contrasting explanations. In principle, it could also be caused by the presence of co-crystallised mixtures of compositionally different $[Ni_{44-x}M_x(CO)_{48}]^{6-}$ (M = Pd or Pt) species giving the observed overall x values. Limited to $[Ni_{24}(Ni_{14-x}Pt_x)Pt_6(CO)_{48}]^{6-}$, the above possibility is excluded by ESI-MS experiments. The observed Ni/Pt disorder can only be caused by the presence in the crystal either of different $[Ni_{35}Pt_9(CO)_{48}]^{6-}$ stereoisomers (molecular disorder), or random orientation of a single stereoisomer (crystal disorder), or an entanglement of both. The latter is clearly the case for $[Ni_{35}Pt_9(CO)_{48}]^{6-}$. Crystal disorder is implied by the presence of a crystallographic centre of symmetry, which cannot be featured by any stereoisomer having an odd number (3) of surface Pt atoms. In view of the differences in the experimental Ni/Pt fractional distributions, the disordered sites may be classified into two distinct groups. A stereoisomer featuring three Pt atoms distributed over the six magenta sites of Figure 3 (either as three neighbouring atoms on one face or as a single and a pair of atoms distributed over two faces) is formally sufficient to interpret the Ni/Pt disordered sites of the first group. A crystallographic

centre of symmetry is assumed to be generated by association in the crystal lattice of the above stereoisomers as such or upside down and mirrored owing to random molecular-ion recognition of the two faces uniquely composed by Ni atoms.

The second group of disordered Ni/Pt sites can be explained by random distribution of three Pt atoms over eight sites (16 independent stereoisomers). As above, these stereoisomers randomly enter the crystal as such and are rotated by 60° and mirrored. An overall occurrence frequency of 86 and 14% of the two groups of stereoisomers would match the experimental Pt fractions.

The formal interpretation of the substitutional Ni/Pd disorder of $[Ni_{36}Pd_8(CO)_{48}]^{6-}$ is straightforward. A single stereoisomer that has two opposite ν_3-triangular faces centred by Pd atoms and has a molecular centre of symmetry is sufficient. This is assumed to enter in the lattice according to the four possible orientations of the idealised C_3 axes of the ν_3-octahedral moiety, with a percentage corresponding to the experimental Pd fraction found in both ions.

Conclusion

The structures of $[Ni_{35}Pt_9(CO)_{48}]^{6-}$ and $[Ni_{36}Pd_8(CO)_{48}]^{6-}$ establish the first similarity between the Ni–Pt and Ni–Pd carbonylated clusters. A comparison between the chemical and electrochemical properties of $[H_{6-n}Ni_{35}Pt_9(CO)_{48}]^{n-}$ and $[H_{6-n}Ni_{38}Pt_6(CO)_{48}]^{n-}$ ($n = 5, 6$) indicates that surface Pt atoms decrease the propensity of the cluster to partially substitute its free negative charge with hydride atoms and limit the range of n values of the non-isoelectronic series of $[Ni_{35}Pt_9(CO)_{48}]^{n-}$ derivatives. Therefore, it seems conceivable to speculate that the truncated octahedral structures of $[Ni_{24}Pt_{14}(CO)_{44}]^{4-}$[7] and $[Pt_{38}(CO)_{44}]^{2-}$[30] directly ensue from a progressive destabilisation of the $[Ni_{44-x}Pt_x]$ ν_3 octahedron as the amount of Pt increases. The effect of Pd seems to be different. The propensity to give several isoelectronic $[H_{6-n}Ni_{36}Pd_8(CO)_{48}]^{n-}$ ($n = 3$–5) hydride derivatives is maintained. However, the probable intrinsic weakness of all bonds involving Pd precludes the possible existence of stable $[Ni_{36}Pd_8(CO)_{48}]^{n-}$ ($n \neq 6$) species.

The different site-selectivity of surface Pd and Pt atoms deserves some comment. Although the carbonyl stereochemistry of the $[Ni_{44-x}M_x(CO)_{48}]^{6-}$ (M = Pt, $x = 6, 9$; M = Pd, $x = 8$) series of compounds is almost identical, coordination with CO of the metal atoms centring the ν_3-triangular faces shows small, but interesting, differences as a function of their Ni, Pd or Pt prevalent identities. Thus, Pd atoms are bonded to three symmetrical face-bridging ligands, Ni atoms bind two symmetrical face-bridging ligands and weakly interacts with an edge-bridging CO (Ni···C = 2.36 Å), and Pt atoms are bonded to one symmetrical and one unsymmetrical triply bridging carbonyl group. The coordination difference between Pd and Ni could probably be caused by the smaller size of the latter and the C···C non-bonding repulsions among three symmetrical three-fold ligands bound to a common Ni atom. Indeed, the C···C and O···O non-bonding contacts of the above three-fold carbonyl groups are in the 2.9–3.1 and 3.1–3.2 Å ranges, respectively. However, the lower coordination of Pt should stem from electronic factors. The coordination of the Ni, Pd and Pt metal atoms centring the ν_3-triangular faces of $[HNi_{38}Pt_6(CO)_{48}]^{5-}$,[5] $[Ni_{24}(Ni_{14-x}Pt_x)Pt_6(CO)_{48}]^{6-}$, $[Ni_{30}(Ni_{8-x}Pd_x)Pd_6(CO)_{48}]^{6-}$, as well as the $[Ni_{24}Pt_{14}(CO)_{44}]^{4-}$[7] and $[Pt_{38}(CO)_{44}]^{2-}$[30] pair of compounds, nicely matches the CO adsorption behaviour of corresponding terrace atoms belonging to close-packed (111) surface layers of Ni, Pd and Pt crystals. At $^1/_3$ CO coverage, both experimental and theoretical results indicate that Pd is bound three-fold, Ni two- and three-fold and Pt on-top of CO, respectively.[31,32] The different coordination preference of CO onto Pd and Pt surfaces seems to be particularly significant to understand Pd and Pt surface segregation in the present clusters. Thus, optimisation of the metal cohesive energy of a bare $[Ni_{36}Pd_8]$ cluster would segregate surface Pd atoms onto the edges. The ν_3-edge atoms of the above clusters display two types of coordination with CO: one edge and two face bridges or one terminal and one face-bridging ligand. The latter coordination seems particularly unlikely for palladium. As a compromise between M–M and M–CO bonding interactions, the Pd atoms are segregated in the centres of the ν_3 faces, preferentially where a coordination with three three-fold carbonyl groups is attainable. In contrast, optimisation of metal cohesive energy in a bare $[Ni_{35}Pt_9]$ cluster would segregate surface Pt atoms in the centres of the ν_3 faces. However, attainment of the most favourable binding properties of Pt with CO would lead these atoms to segregate onto the ν_3-edge sites of the second type or in the lowest CO-coordinated face-centring sites, as experimentally observed. Therefore, the observed surface segregation of Pd and Pt in the above carbonyl clusters seems to derive from a subtle compromise between optimisation of M–M and M–CO interactions and could be of some significance in interpreting metal migration, chemiadsorption and catalytic behaviour of Ni–Pd and Ni–Pt alloy particles.[29,32]

Experimental Section

All reactions and sample manipulations were carried out using standard Schlenk techniques under nitrogen and in dried solvents. The $[Ni_6(CO)_{12}]^{2-}$ salts have been prepared according to the literature.[33] Analyses of Ni, Pd and Pt were performed by atomic absorption on a Pye-Unicam instrument. Analyses of C, H and N were obtained with a ThermoQuest FlashEA 1112 NC instrument. IR spectra were recorded on a Perkin Elmer 1605 interferometer in CaF_2 cells. Proton NMR spectra were recorded on a Varian Gemini 300 MHz instrument, and ESI mass spectra were determined on a Waters Micromass ZQ 4000 instrument. Materials and apparatus for electrochemistry have been described elsewhere.[6] The figures were drawn with SCHAKAL 99.[34]

Synthesis of $[NBu_4]_6[Ni_{35}Pt_9(CO)_{48}]$: $[Pt(SEt_2)_2Cl_2]$ (1.20 g, 2.7 mmol) was added in portions to a solution of $[NBu_4]_2[Ni_6(CO)_{12}]$ (2.62 g, 2.24 mmol) in ethyl acetate (60 mL) with stirring. The mixture was left to react for 48 h, and the resulting dark brown suspension was filtered and evaporated to dryness. The residue was thoroughly washed with water (40 mL) and then with isopropyl alcohol (30 mL). The residual brown material was extracted in THF (30 mL) and then in acetone (50 mL). The THF solution afforded black plates of $[NBu_4]_6[Ni_{35}Pt_9(CO)_{48}]\cdot 6\,THF$ on standing ($\approx$0.08 g). An additional 1.10 g of $[NBu_4]_6[Ni_{35}Pt_9(CO)_{48}]\cdot x\,Me_2CO$ was precipitated from the acetone solution by treating it with a few drops

of sodium methoxide in methanol followed by layering with *n*-heptane (40 mL). The overall yield was ≈60% based on Pt. The salt is soluble in acetone, acetonitrile, DMF, DMSO, less soluble in THF, sparingly soluble in alcohols and insoluble in non-polar solvents. Elemental analysis calcd (%) for $[NBu_4]_6[Ni_{35}Pt_9(CO)_{48}]\cdot 6\,THF$: C 28.65, H 3.78, N 1.19, Ni 29.17, Pt 24.93; found: C 28.53, H 3.86, N 1.14, Ni 28.87, Pt 24.52.

Synthesis of $[NBu_4]_6[Ni_{36}Pd_8(CO)_{48}]$: $[Pd(SEt_2)_2Cl_2]$ (0.82 g, 2.29 mmol) was added in portions to a solution of $[NBu_4]_2[Ni_6(CO)_{12}]$ (2.06 g, 1.76 mmol) in THF (60 mL) under a continuously renewed nitrogen atmosphere. The mixture was stirred for 6 h, and then left to react for three days as above. The resulting dark brown suspension was filtered and evaporated to dryness. The residue was thoroughly washed with water (40 mL) and then with isopropyl alcohol (30 mL). The residual brown material was extracted in acetone (20 mL) and partially precipitated by layering with isopropyl alcohol (20 mL) to obtain the known $[NBu_4]_4[Ni_{16}Pd_{16}(CO)_{40}]$ salt. The mother liquor was dried under vacuum, and the residue was repeatedly crystallised from acetone and *n*-hexane to obtain black plates of $[NBu_4]_{12}[Ni_{30}(Ni_{8-x}Pd_x)Pd_6(CO)_{48}][Ni_{30}(Ni_{8-x'}Pd_{x'})Pd_6(CO)_{48}]\cdot 6\,(CH_3)_2CO\cdot C_6H_{14}$ (x and $x' = 2$) (81 mg, 5% based on Pd). The salt is soluble in THF, acetone, acetonitrile, DMF, DMSO, sparingly soluble or insoluble in alcohols and non-polar solvents. Elemental analysis calcd for $[NBu_4]_6[Ni_{36}Pd_8(CO)_{48}]\cdot 3\,(CH_3)_2CO\cdot 0.5\,C_6H_{14}$: C 31.33, H 4.06, N 1.41, Ni 35.33, Pd 14.24; found: C 31.21, H 3.97, N 1.32, Ni 35.18, Pd 14.62.

X-ray studies: Crystal data and collection details for $[NBu_4]_6[[Ni_{24}(Ni_{14-x}Pt_x)Pt_6(CO)_{48}]\cdot 6\,THF$ ($x = 3$) and $[NBu_4]_{12}[Ni_{30}(Ni_{8-x}Pd_x)Pd_6(CO)_{48}][Ni_{30}(Ni_{8-x'}Pd_{x'})Pd_6(CO)_{48}]\cdot 6\,(CH_3)_2CO\cdot C_6H_{14}$ (x and $x' = 2$) are reported in Table 4. The diffraction experiments were carried out on a Bruker SMART2000 diffractometer equipped with a CCD detector at room temperature for $[NBu_4]_6[[Ni_{24}(Ni_{14-x}Pt_x)Pt_6(CO)_{48}]\cdot 6\,THF$ ($x = 3$) and at −50 °C for $[NBu_4]_{12}[Ni_{30}(Ni_{8-x}Pd_x)Pd_6(CO)_{48}][Ni_{30}(Ni_{8-x'}Pd_{x'})Pd_6(CO)_{48}]\cdot 6\,(CH_3)_2CO\cdot C_6H_{14}$ (x and $x' = 2$). Data were corrected for Lorentz polarisation and absorption effects (empirical absorption correction SADABS).[35] The structures were solved by direct methods and refined with full-matrix least-squares (SHELX97[36]) for independent reflections with $I > 2\sigma(I)$. In the case of the $[NBu_4]_{12}[Ni_{30}(Ni_{8-x}Pd_x)Pd_6(CO)_{48}][Ni_{30}(Ni_{8-x'}Pd_{x'})Pd_6(CO)_{48}]\cdot 6\,(CH_3)_2CO\cdot C_6H_{14}$ (x and $x' = 2$) salt , on account of the extremely high number of parameters to refine, the data set was divided into two blocks, one including the anionic parts, the other including the cations and the solvent molecules. For both species, the disordered metal sites were initially refined isotropically with coordinate and displacement parameter restraints in order to obtain the relative occupancy factors. Preliminary refinement of $[NBu_4]_6[[Ni_{24}(Ni_{14-x}Pt_x)Pt_6(CO)_{48}]\cdot 6\,THF$ gave a non-integer stoichiometry ($x = 3.29$); in accordance with the experimental indication from ESI-MS, the occupancy factors of disordered Ni/Pt metal sites were restrained to have an overall x value of 3.0. Analogously, the first refinement of $[NBu_4]_{12}[Ni_{30}(Ni_{8-x}Pd_x)Pd_6(CO)_{48}][Ni_{30}(Ni_{8-x'}Pd_{x'})Pd_6(CO)_{48}]\cdot 6\,(CH_3)_2CO\cdot C_6H_{14}$ afforded x and x' values of 1.98 and 2.4, respectively. Two independent sites of each anion (orange spheres in Figure 5) featured Pd fraction < 0.1. The second refinement as $[NBu_4]_{12}[Ni_{34}(Ni_{4-x}Pd_x)Pd_6(CO)_{48}][Ni_{34}(Ni_{4-x'}Pd_{x'})Pd_6(CO)_{48}]\cdot 6\,(CH_3)_2CO\cdot C_6H_{14}$, in which those sites were treated as pure Ni atoms gave x and x' values of 1.60 and 1.94, respectively. A third refinement model, in which all eight disordered Ni/Pd sites were constrained to with $x = 2.0$, gave a slightly improved fitting, and this was used in subsequent refinements. After fixing the occupancy factors, all metal sites, including the disordered ones, were anisotropically refined keeping coordinate and displacement parameter restraints. Anisotropic displacement parameters were also assigned to all other atoms of the anions and cations, while solvent molecules were treated as isotropic. CCDC-211556 and CCDC-211557 contain the supplementary crystallographic data for $[NBu_4]_6[[Ni_{24}(Ni_{14-x}Pt_x)Pt_6(CO)_{48}]\cdot 6\,THF$ ($x = 3$) and $[NBu_4]_{12}[Ni_{30}(Ni_{8-x}Pd_x)Pd_6(CO)_{48}][Ni_{30}(Ni_{8-x'}Pd_{x'})Pd_6(CO)_{48}]\cdot 6\,(CH_3)_2CO\cdot C_6H_{14}$ (x and $x' = 2$), respectively. These data can be obtained free of charge via www.ccdc.cam.ac.uk/conts/retrieving.html (or from the Cambridge Crystallographic Data Centre, 12 Union Road, Cambridge CB2 1EZ, UK; fax: (+44) 1223-336033; or deposit@ccdc.cam.uk).

Table 4. Crystal data and structure refinement for $[NBu_4]_6[Ni_{24}(Ni_{14-x}Pt_x)Pt_6(CO)_{48}]\cdot 6\,THF$ ($x = 3$) and $[NBu_4]_{12}[Ni_{30}(Ni_{8-x}Pd_x)Pd_6(CO)_{48}][Ni_{30}(Ni_{8-x'}Pd_{x'})Pd_6(CO)_{48}]\cdot 6\,(CH_3)_2CO\cdot C_6H_{14}$ (x and $x' = 2$).

empirical formula	$C_{168}H_{264}N_6Ni_{35}O_{54}Pt_9$	$C_{156}H_{241}N_6Ni_{36}O_{51}Pd_8$
formula weight	7042.51	5981.31
T [K]	293(2)	223(2)
λ [Å]	0.71073	0.71073
crystal system	monoclinic	triclinic
space group	$P2(1)/n$	$P\bar{1}$
a [Å]	19.071(1)	18.124(1)
b [Å]	19.285(1)	18.261(1)
c [Å]	31.363(2)	31.876(2)
α [°]	90	92.87(1)
β [°]	102.89(1)	100.19(1)
γ [°]	90°	90.78(1)
V [Å^3]	11244.2(15)	10367.8(13)
Z	2	2
ρ_{calcd} [Mg m^{-3}]	2.080	1.916
μ [mm^{-1}]	8.486	3.918
$F(000)$	6856	6006
crystal size [mm]	0.20 × 0.15 × 0.10	0.15 × 0.15 × 0.10
θ range for data collection [°]	1.15–30.26	3.02–30.00
index ranges	$-26 \le h \le 26$ $-23 \le k \le 26$ $-43 \le l \le 42$	$-21 \le h \le 21$ $-21 \le k \le 21$ $-37 \le l \le 37$
reflns collected	79098	81148
independent reflns, R(int)	29959, 0.0982	36398, 0.0467
absorption correction	empirical	empirical
max./min. transmission	0.4841/0.2816	0.6953/0.5079
refinement method	full-matrix least-squares on F^2	full-matrix least-squares on F^2
data/restraints/parameters	29959/142/1140	36398/531/2239
GOOF on F^2	1.017	1.129
final R indices $[I > 2\sigma(I)]$		
$R1$	0.0816	0.0589
$wR2$	0.1976	0.1655
R indices (all data)		
$R1$	0.1765	0.1097
$wR2$	0.2766	0.1849
largest diff. peak and hole [e Å^{-3}]	3.605/−3.010	1.847/−1.107

Acknowledgments

Financial support from the University of Bologna (Italy) and the MIUR (COFIN2003) is gratefully acknowledged. G.L. thanks Prof. V. G. Albano for helpful discussions and Luca Zuppiroli for technical assistance with the ESI mass spectra.

[1] N. T. Tran, M. Kawano, D. R. Powell, L. F. Dahl, *J. Chem. Soc. Dalton Trans.* **2000**, 4138–4144.
[2] C. Femoni, M. C. Iapalucci, G. Longoni, P. H. Svensson, J. Wolowska, *Angew. Chem.* **2000**, *112*, 1702–1704; *Angew. Chem. Int. Ed.* **2000**, *39*, 1635–1636.
[3] F. Demartin, C. Femoni, M. C. Iapalucci, G. Longoni, P. Macchi, *Angew. Chem.* **1999**, *111*, 552–554; *Angew. Chem. Int. Ed.* **1999**, *38*, 531–533.
[4] F. Demartin, F. Fabrizi de Biani, C. Femoni, M. C. Iapalucci, G. Longoni, P. Macchi, P. Zanello, *J. Cluster Sci.* **2001**, *12*, 61–74.
[5] A. Ceriotti, F. Demartin, G. Longoni, M. Manassero, M. Marchionna, G. Piva, M. Sansoni, *Angew. Chem.* **1985**, *97*, 708–709; *Angew. Chem. Int. Ed. Engl.* **1985**, *24*, 697–698.

[6] F. Fabrizi de Biani, C. Femoni, M. C. Iapalucci, G. Longoni, P. Zanello, A. Ceriotti, *Inorg. Chem.* **1999**, *38*, 3721–3724.
[7] C. Femoni, M. C. Iapalucci, G. Longoni, P. H. Svensson, *Chem. Commun.* **2001**, 1776–1777.
[8] M. Kawano, J. W. Bacon, C. F. Campana, L. F. Dahl, *J. Am. Chem. Soc.* **1996**, *118*, 7869–7870.
[9] M. Kawano, J. W. Bacon, C. F. Campana, B. E. Winger, J. D. Dubek, S. A. Sirchio, S. L. Skruggs, U. Geiser, L. F. Dahl, *Inorg. Chem.* **2001**, *40*, 2554–2569.
[10] J. M. Bemis, L. F. Dahl, *J. Am. Chem. Soc.* **1997**, *119*, 4545–4546.
[11] G. Longoni, M. C. Iapalucci in *Clusters and Colloids - From Theory to Applications* (Ed.: G. Schmid), VCH, **1994**, pp. 89–177.
[12] R. W. Broach, L. F. Dahl, G. Longoni, P. Chini, A. J. Schultz, J. M. Williams in *Transition Metal Hydride* (Ed.: R. Bau), *Adv. Chem. Ser.* **1978**, *167*, 93–110.
[13] A. Ceriotti, F. Demartin, G. Longoni, M. Manassero, G. Piva, G. Piro, M. Sansoni, B. T. Heaton, *J. Organomet. Chem.* **1986**, *301*, C5–C8.
[14] A. Ceriotti, P. Chini, R. Della Pergola, G. Longoni, *Inorg. Chem.* **1983**, *22*, 1595–1598.
[15] M. Marchionna, PhD Thesis, University of Milano, **1986**.
[16] N. T. Tran, M. Kawano, R. K. Hayashi, D. R. Powell, C. F. Campana, L. F. Dahl, *J. Am. Chem. Soc.* **1999**, *121*, 5945–5952.
[17] D. Collini, C. Femoni, M. C. Iapalucci, G. Longoni, P. Zanello, in *Perspectives in Organometallic Chemistry* (Eds.: C. G. Screttas, B. R. Steele), RSC Books, **2003**, *287*, 183–195.
[18] D. Collini, C. Femoni, M. C. Iapalucci, G. Longoni, P. H. Svensson, P. Zanello, *Angew. Chem.* **2002**, *114*, 3837–3840; *Angew. Chem. Int. Ed.* **2002**, *41*, 3685–3688.
[19] L. F. Dahl, cited in ref. [1]
[20] J. C. Traeger, *Int. J. Mass Spectrom.* **2000**, *200*, 387–401.
[21] B. F. G. Johnson, J. S. McIndoe, *Coord. Chem. Rev.* **2000**, *200*, 901–932.
[22] C. E. C. A. Hop, R. Bakhtiar, *J. Chem. Educ.* **1996**, *73*, A162-A169.
[23] P. J. Dyson, A. K. Hearley, B. F. G. Johnson, J. S. McIndoe, P. Langridge-Smith, *J. Cluster Sci.* **2001**, *12*, 273–283.
[24] P. J. Dyson, N. Feeder, B. F. G. Johnson, J. S. McIndoe, P. R. R. Langridge-Smith, *J. Chem. Soc. Dalton Trans.* **2000**, 1813–1815.
[25] P. J. Dyson, B. F. G. Johnson, J. S. McIndoe, P. Langridge-Smith, *Inorg. Chem.* **2000**, *39*, 2430–2431.
[26] Y. Gauthier, Y. Joly, R. Baudoing, J. Rundgren, *Phys. Rev. B* **1985**, *31*, 6216–6218.
[27] Y. Gauthier, R. Baudoing, M. Lundberg, J. Rundgren, *Phys. Rev. B* **1987**, *35*, 7867–7878.
[28] M. Lundberg, *Phys. Rev. B* **1987**, *36*, 4692–4699.
[29] J. A. Rodriguez, *Surf. Sci. Rep.* **1996**, *24*, 223–287, and references therein.
[30] A. Ceriotti, N. Masciocchi, P. Macchi, G. Longoni, *Angew. Chem.* **1999**, *111*, 3941–3944; *Angew. Chem. Int. Ed.* **1999**, *38*, 3724–3727.
[31] Y-T. Wong, R. Hoffmann, *J. Phys.Chem.* **1991**, *95*, 859–867, and references therein.
[32] P. H. T. Philipsen, E. Van Lenthe, J. G. Snijders, E. J. Baerends, *Phys. Rev.* B **1997**, *56*, 13556–13562.
[33] A. C. Michel, L. Lianos, J. L. Rousset, P. Delichere, N. S. Prakash, J. Massardier, Y. Jugnet, J. C. Bertolini, *Surf. Sci.* **1998**, *416*, 288–294.
[34] H. Keller, SCHAKAL 99, University of Freiburg (Germany), **1999**.
[35] G. M. Sheldrick, SADABS, University of Göttingen, Germany.
[36] G. M. Sheldrick, SHELX97-Program for the refinement of Crystal Structure, University of Göttingen,Göttingen (Germany), **1997**.

Received: June 10, 2003
Revised: December 30, 2003 [F5210]